Table of Contents

a.

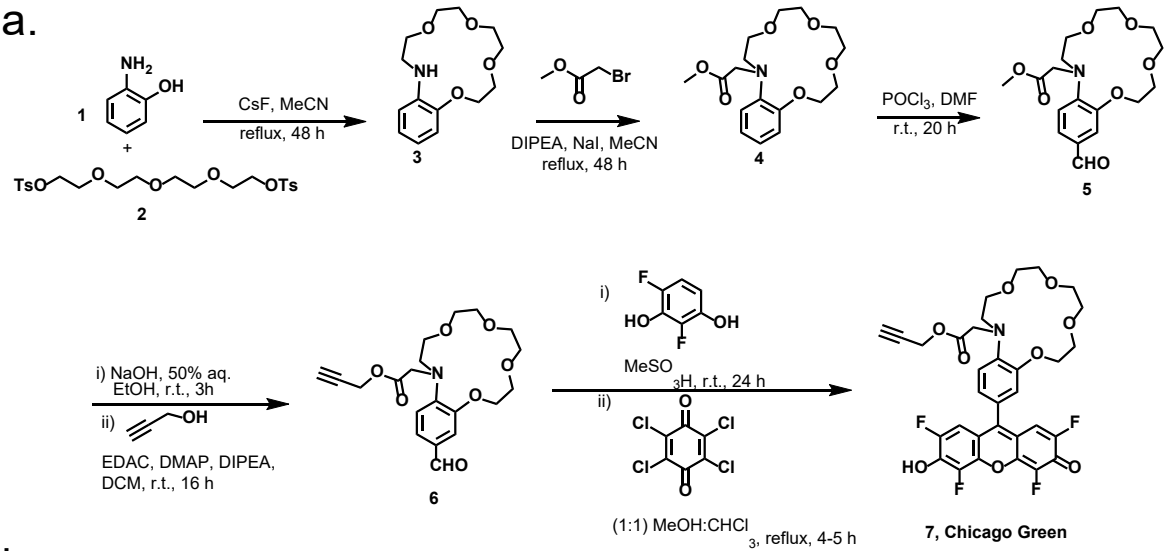

b.

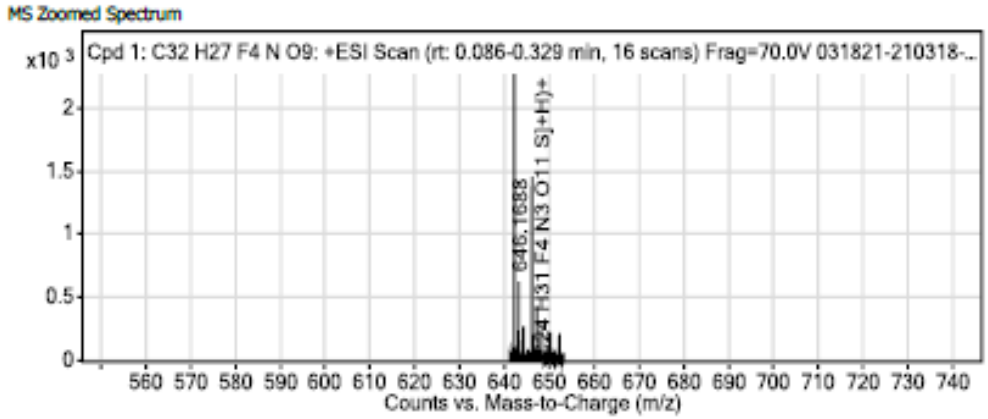

MS Spectrum Peak List

Obs. m/z	Charge	Abund	Formula	Ion/Isotope	Tgt Mass Error (ppm)
646.1688	1	1458.38	C24 H31 F4 N3 O11 S	(M+H)+	0.06
647.1728	1	432.11	C24 H31 F4 N3 O11 S	(M+H)+	-1.39
648.1883	1	203.61	C24 H31 F4 N3 O11 S	(M+H)+	-27.91

Supplementary Figure 1. Synthesis of Chicago Green

a. Synthesis scheme of Chicago Green dye. Detailed steps are included in Supplementary note 1. b. High Resolution Mass Spectrometry analysis for Chicago Green dye. m/z is identical to protonated Chicago Green dye.

Supplementary Note 1. Synthesis of Chicago Green

A brief description of synthetic methods is provided below. Compounds 3-5 were synthesized following previously reported methods[1]:

Synthesis of 1-aza-benzo-15-crown-5 ether, ***3***. A mixture of 2-aminophenol, **1** (1 g, 9 mmol) and cesium fluoride (7 g, 45 mmol) in acetonitrile (800 mL) was stirred vigorously for 2 h under nitrogen

atmosphere. Next, tetraethylene gycol di(p-toluenesulfonate), **2** (4.57 g, 3.6 mL, 9 mmol) in 50 mL acetonitrile was added to the solution and refluxed under nitrogen atmosphere for 48 h. The solution was allowed to cool down to room temperature and then evaporated using a rotavac. The residue was dissolved in chloroform (600 mL) and filtered. The chloroform layer was then washed with water (200 mL), saturated sodium bicarbonate (200 mL), brine (200 mL), and evaporated using a rotavac. The residue was subjected to silica gel column chromatography (50-70% ethyl acetate/hexane) to obtain pure **3** (1.1 gm, 4.1 mmol, yield ~45%) as a yellowish-brown oil. ESI-MS: calculated m/z for [**3**+H^+] = 268.15, observed m/z = 268.2. ^{1}H NMR (400 MHz, $CDCl_3$, δ ppm): 6.89-6.85 (t, 1H, J_1=J_2=8 Hz), 6.77-6.75 (d, 1H, J=8 Hz), 6.64-6.58 (dd, 2H, J_1=16 Hz, J_2=J_3=8 Hz), 5.13 (b, 1H), 4.12-4.09 (m, 2H), 3.86-3.84 (t, 2H, J_1=J_2=4 Hz), 3.80-3.77 (t, 2H, J_1=4 Hz, J_2=8 Hz), 3.73-3.67 (m, 8H), 3.26-3.24 (t, 2H, J_1=J_2=4 Hz). ^{13}C NMR (100 MHz, $CDCl_3$, δ ppm): 146.4, 139.6, 121.9, 116.4, 112.0, 110.3, 70.4, 70.0, 69.9, 69.5, 69.0, 68.3, 43.3. ESI-MS (m/z for [**3**+H^+]): Calculated, 268.15; Observed, 268.2.

*Synthesis of **4***. Compound **3** (1.0 gm, 3.7 mmol), methyl bromoacetate (1.14 g, 0.7 mL, 7.5 mmol), DIPEA (2.4 g, 3.3 mL, 18.7 mmol) and sodium iodide (0.55 g, 3.7 mmol) were taken in dry acetonitrile (30 mL) and refluxed for 48 h under nitrogen atmosphere. The reaction mixture was allowed to reach room temperature and the solvent was evaporated using a rotavac. The residue was dissolved in dichloromethane (100 mL) and washed with water (20 mL). The organic layer was dried with anhydrous magnesium sulfate, filtered and evaporated using a rotavac. The crude product was subjected to silica gel column chromatography (0-8% methanol/dichloromethane) to obtain compound **4** (0.9 g, 2.6 mmol, yield ~71%). ^{1}H NMR (400 MHz, $CDCl_3$, δ ppm): 6.97-6.94 (m, 1H), 6.89-6.85 (m, 2H), 6.82-6.80 (m, 1H), 4.14-4.12 (m, 4H), 3.90-3.88 (m, 2H), 3.77-3.73 (m, 4H), 3.70-3.66 (m, 11 H).

*Synthesis of **5***. $POCl_3$ (1.97 g, 1.2 mL, 12.9 mmol) was slowly added to dry DMF (1 mL) under ice-cold condition and nitrogen atmosphere to form the Vilsmeier's reagent. Compound **4** (0.9 g, 2.64 mmol) dissolved in dry DMF (0.7 mL) was slowly added to the Vilsmeier's reagent and the reaction mixture was stirred for 24 h at room temperature under nitrogen atmosphere. The solution was then slowly poured into a mixture of ice-cold saturated potassium carbonate solution (50 mL). Water (25 mL) was added and the aqueous solution was extracted with dichloromethane (20 mL, 5x). The combined organic extract was dried with anhydrous sodium sulfate, filtered and evaporated using a rotavac. The crude product was subjected to silica gel column chromatography (0-8% methanol/dichloromethane) to obtain compound **5** (0.74 g, 2.0 mmol, yield ~76%) as a yellow oil. ^{1}H NMR (400 MHz, $CDCl_3$, δ ppm): 9.75 (s, 1H), 7.35-7.32 (m, 2H), 6.79-6.77 (d, 1H, J=8 Hz), 4.26 (s, 2H), 4.21-4.19 (m, 2H), 3.91-3.87 (m, 4H), 3.72 (s, 3H), 3.69-3.65 (m, 10H). ^{13}C NMR (100 MHz, $CDCl_3$, δ ppm): 190.0, 171.0, 149.8, 145.8, 128.8, 126.0, 116.4, 111.0, 70.6, 69.9, 69.7, 69.3, 68.9, 68.4, 53.1, 52.0, 51.4. ESI-MS (m/z for [**5**+H^+]): Calculated, 368.17; Observed, 368.1.

*Synthesis of **6***. Compound **5** (0.74 g, 2.0 mmol) and sodium hydroxide (0.24 g, 6.0 mmol) were dissolved in 50% aqueous ethanol (8 mL) and stirred at room temperature for 2.5 h. Next, the solution was neutralized with 3N HCl and ethanol was evaporated using rotavac. The concentrate was diluted with water (30 mL) and extracted with dichloromethane (20 mL, 5x). The combined organic extracts were washed with brine (20 mL, 1x), dried over anhydrous sodium sulfate, filtered, and evaporated to dryness using a rotavac. The obtained residue (0.55 g) was used in the next

step without any purification. The crude residue, along with propargyl alcohol (0.13 g, 0.13 mL, 2.31 mmol), DIPEA (0.3 g, 0.4 mL, 2.3 mmol), and DMAP (37 mg, 0.31 mmol) were dissolved in dry dichloromethane (10 mL) and the solution was cooled in an ice bath. EDC (0.44 g, 2.3 mmol) was added to it and the reaction was stirred at room temperature for 16 h. On reaction completion, the solution was diluted with dichloromethane (30 mL), washed with water (20 mL, 2x) and brine (20 mL, 2x), dried over anhydrous sodium sulfate, filtered, and evaporated using a rotavac. The obtained crude residue was subjected to silica gel column chromatography (0-5% methanol/dichloromethane) to obtain **6** (0.46 g, 1.2 mmol, ~59% yield) as a yellow viscous oil. ^{1}H NMR (400 MHz, $CDCl_3$, δ ppm): 9.77 (s, 1H), 7.36-7.33 (m, 2H), 6.83-6.81 (d, 1H, *J*=8 Hz), 4.74-4.73 (d, 2H, *J*=4 Hz), 4.35 (s, 2H), 4.22-4.20 (m, 2H), 3.91-3.88 (m, 4H), 3.72-3.66 (m, 11H). ^{13}C NMR (100 MHz, $CDCl_3$, δ ppm): 189.6, 169.3, 149.3, 144.9, 128.4, 125.7, 116.3, 110.3, 76.3, 74.4, 70.0, 69.6, 69.4, 69.2, 69.1, 68.6, 68.2, 67.6, 52.5, 51.5, 51.2. ESI-MS (m/z for [**6**+H^+]): Calculated, 392.17; Observed, 392.2.

Synthesis of Chicago Green, ***7***. Compound **6** (132 mg, 0.34 mmol), 2,4-difluororesorcinol (98.5 mg, 0.67 mmol) and methanesulfonic acid (3 mL) was stirred at room temperature for 48 h under nitrogen atmosphere. The reaction mixture was diluted with water (2 mL) and slowly poured into ice-cold sodium acetate solution (3N, 15 mL) and extracted with ethyl acetate (20 mL, 5x). The combined organic extract was dried with anhydrous sodium sulfate, filtered and evaporated using a rotavac. The obtained crude solid (200 mg) and chloranil (300 mg, 1.2 mmol) was taken in 1:1 chloroform/methanol (15 mL) and refluxed for 4-5 h. The reaction mixture was cooled, filtered and evaporated using a rotavac. The residue was subjected to reverse phase HPLC using 1:1 methanol/acetonitrile as the eluent to obtain **7** (2.5 mg, 3.9 nmol, yield ~11%). QTOF-HRMS (m/z for [**7**+H^+]): Calculated, 646.1695; Observed, 646.1688.

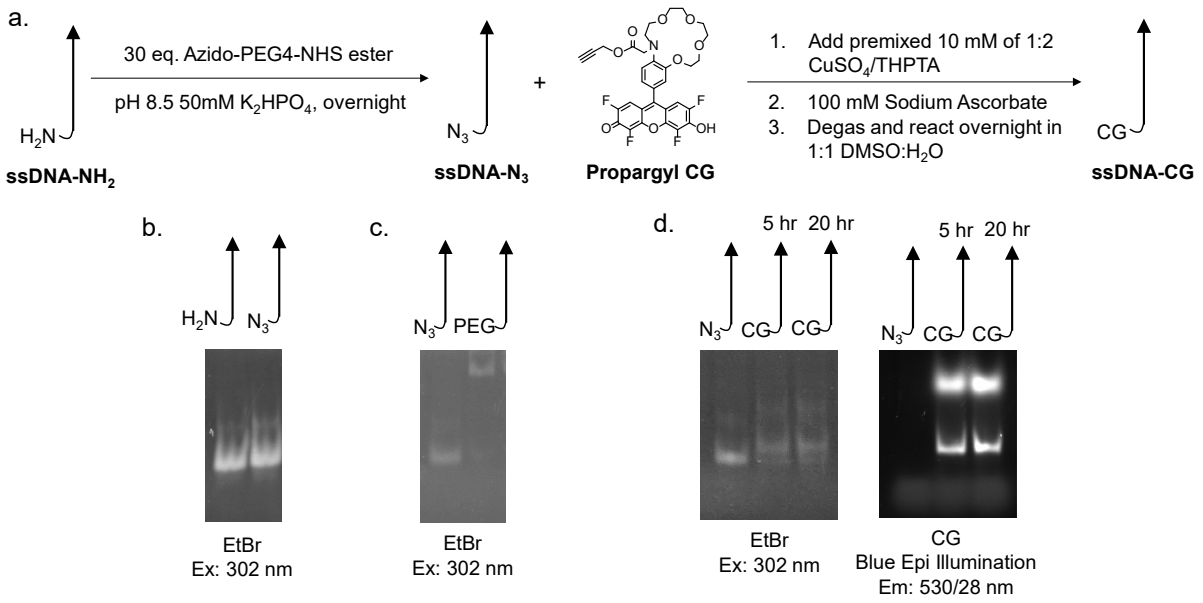

Supplementary Figure 2. Conjugation of CG to DNA
a. Reaction scheme of CuAAC coupling of CG to ssDNA. b-d. native PAGE of DNA intermediates and products. Unlabeled DNA strands are visualized with EtBr staining and CG conjugated DNA strand is visualized with fluorescence. Gel is representative of n = 2 independent experiments.

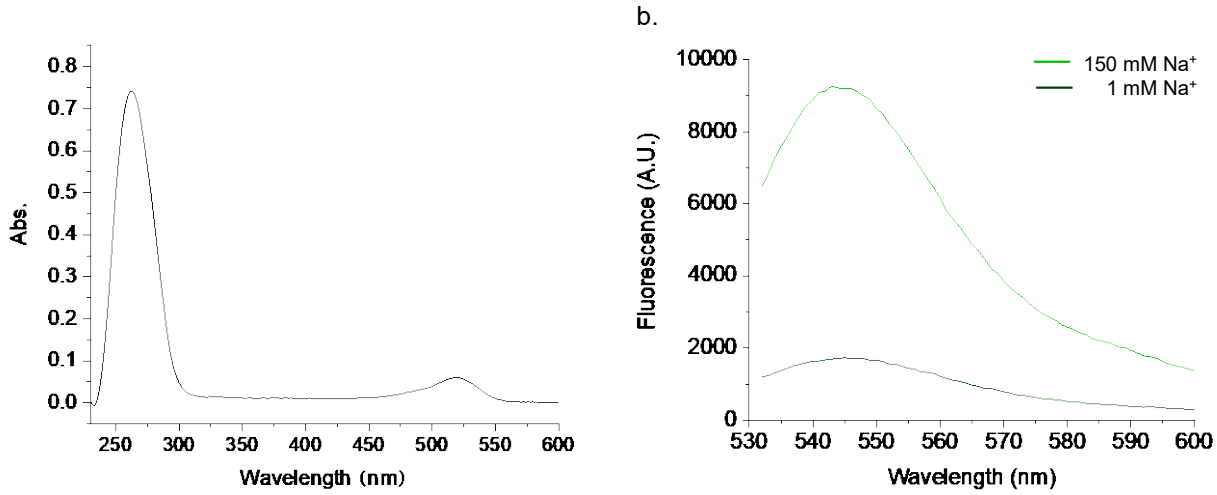

Supplementary Figure 3. Validation of CG-DNA conjugate efficiency and Na^+ sensitivity
a. UV-Vis spectrum of ssDNA-CG. Molar ratio of DNA to CG is confirmed to be ~ 1:1 confirming the coupling efficiency. b. ssDNA-CG fluorescence increases with high Na^+. 1mM and 150mM NaCl was added to 100nM of ssDNA-CG in pH 7.4 potassium phosphate buffer. Fluorescence maximum at 545 increases more than 5-fold.

Supplementary Note 2. CG conjugation and validation.

25mer 5'-amine with C6 linker modified DNA was purchased (IDT) and quantified by 260 nm absorption. ssDNA-NH_2 was converted to ssDNA-N_3 by NHS ester activated crosslinking. DNA was then ethanol precipitated from reaction mix and washed with 70% EtOH. In 12% native PAGE ssDNA-NH_2 and ssDNA-N_3 have similar gel shift as seen in **Supplementary Fig 2b**. CG dye CuAAC coupling to ssDNA-N_3 was done by first premixing 10mM / 20mM $CuSO_4$/THPTA for ligand chelation. Add copper catalyst mix to DNA and propargyl CG. Finally add freshly dissolved 100 mM sodium ascorbate and purge the reaction mix with nitrogen gas for 3 min. Wrap the tube with parafilm and stir to react overnight at room temperature. Reaction mix was taken at 5 hr and 20 hr and ran by 12% native PAGE. Fluorophore coupling was confirmed by the lower fluorescent DNA band. Upper band in fluorescence channel disappeared after ethanol precipitation. The precipitate has intense pink color.

To confirm full conversion of ssDNA-NH_2 to ssDNA-N_3, a small aliquot of ssDNA-N_3 was taken and reacted with 10k Da DBCO-PEG to make ssDNA-PEG. We used this strategy because DBCO and azide can react to completion and bulky 10k Da PEG can alter the gel shift (Supplementary Figure 2c).

To confirm full conversion of ssDNA-N_3 to ssDNA-CG, absorption spectra was taken for the conjugate (**Supplementary Fig 3a**). ϵ = 251,000 L / (mole·cm) for 25 mer ssDNA at 260 nm. ϵ = 21,000 L / (mole·cm) for CG at 522 nm. All free CG dye is excluded from EtOH precipitation and the calculated molar ratio of CG peak and DNA peak shows is ~1:1.

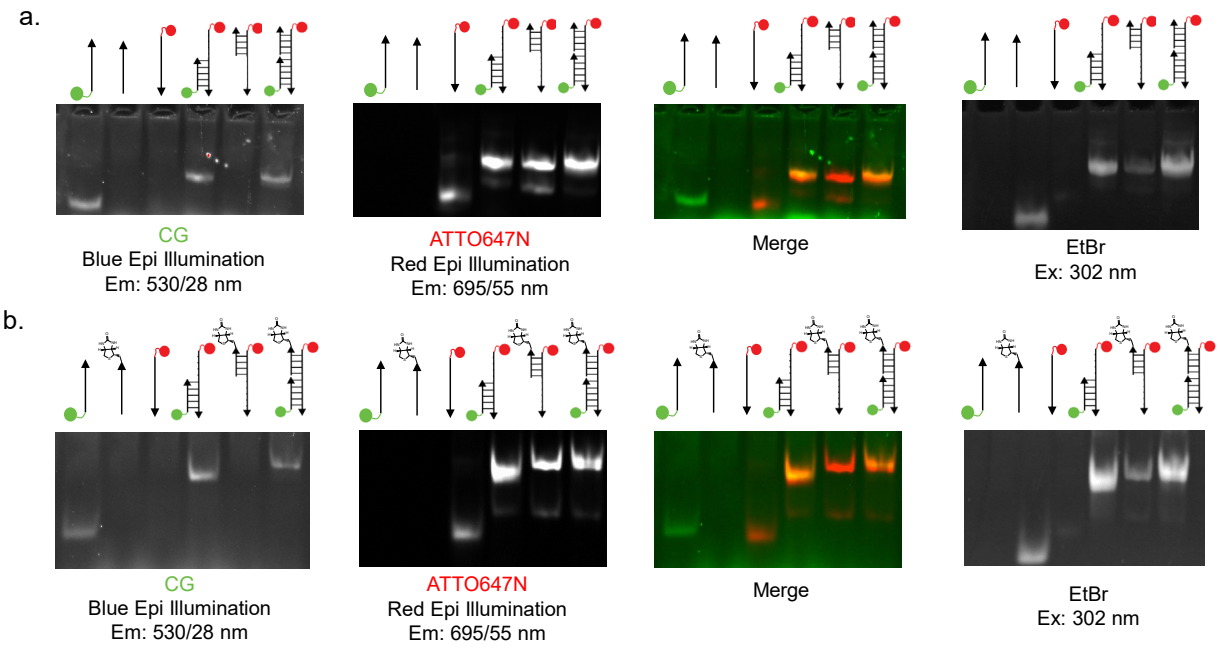

Supplementary Figure 4. Gel eletrophoresis of *RatiNa* sensors
a. 12% native PAGE of *RatiNa* sensor. b. 12% native PAGE for biotinylated *RatiNa*^{biotin}. Arrowed line represents ssDNA, green circle represents CG dye and red circle represents ATTO dye. Gels are representative of n = 2 independent experiments.

Supplementary Note 3. PAGE analysis of *RatiNa* sensors
We used 12% native PAGE to check the annealed *RatiNa* sensors. Gel was run at 100 V for 45 minutes. All three single strands and partial annealed products are run together. All three single strands have significantly different gel shift and not present in the annealed sample. The partial annealed products have a slight gel shift compared to *RatiNa* and both products are not seen in annealed sample. And the annealed sensor contains both CG dye and normalizing dye by showing both red and green fluorescence.

Biotinylated *RatiNa* sensor was made with same two fluorescent ssDNA and a 3'-biotin modified ssDNA (IDT). Similarly, *RatiNa*^{biotin} contains both CG dye and normalizing dye by showing both red and green fluorescence and no partially annealed products.

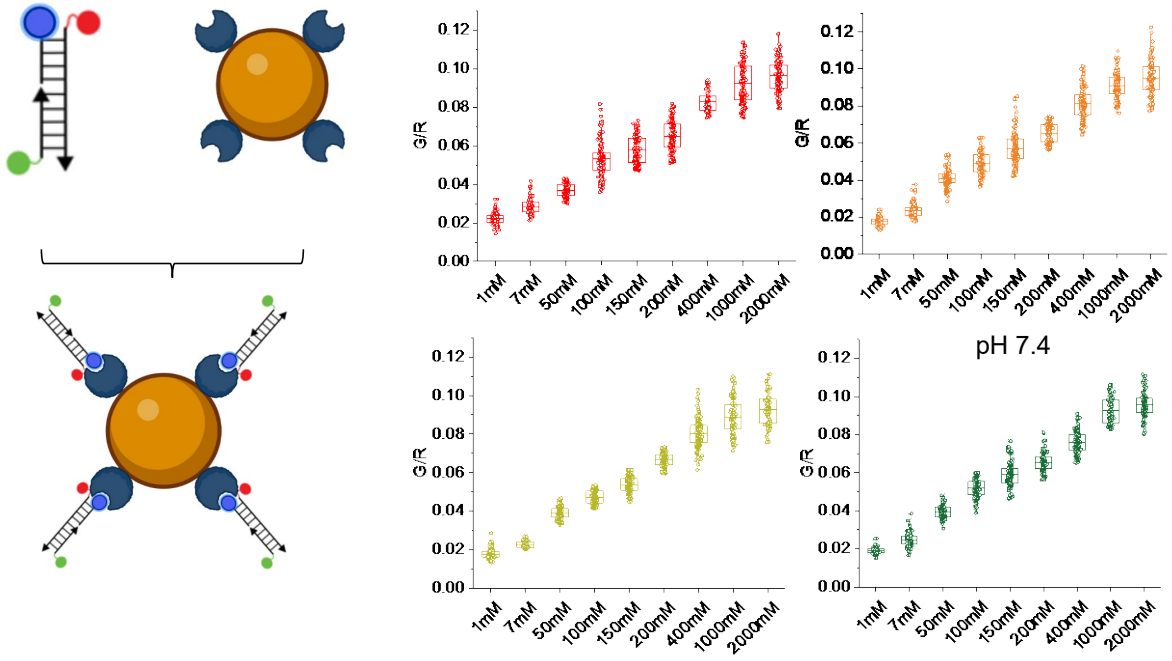

Supplementary Figure 5. Bead calibration of *RatiNa* sensors

a. scheme of making *RatiNa* bead. *RatiNa*^{biotin} was added to streptavidin bound bead. Beads were around the size of organelle and can be imaged in any buffer of choice for microscopy characterization. a-d. *RatiNa* bead was imaged in pH = 4.5, 5.5, 6.5 and 7.4 Na^+ calibration buffer and imaged with widefield microscope (n = 54 – 172, 87 – 224, 63 – 297, 88 – 186 beads for pH 4.5, 5.5, 6.5, 7.4. median line was shown, box represents 25% and 75% percentile, error bar represents 95% and 5% percentile).

Supplementary Note 4. Na^+ and pH response of *RatiNa* on beads

To fully characterize *RatiNa* in terms of Na^+ affinity, pH insensitivity and selectivity, we decided to use fluorescent imaging method since the fluorescence signal is the final read out. Thus, we can image *RatiNa* with same image acquisition settings as we use for both in vitro characterization and in vivo measurement. To image *RatiNa* we use the biotinylated *RatiNa* to coat streptavidin bead with *RatiNa* and image the bead in various buffer conditions. In brief, 1 µm streptavidin coated polystyrene bead (Bangs Laboratories, CP01004) was first washed twice and then incubated with 10 µM of $RatiNa^{biotin}$ in phosphate buffer. Either vigorous shaking or magnetic stirrers can be used to keep beads well mixed. After 2 hours of shaking the bead can be collected by centrifuging at 5,000 rpm and stored in phosphate buffer. 0.1% Tween-20 was added to prevent aggregation of beads.

Beads were then imaged to test Na^+ response. *RatiNa* beads were resuspended in Na^+ buffer (1 mM to 2000mM NaCl, 10 mM HEPES, 10 mM MES, 10 mM KOAc. pH from 4.5 to 7.4 adjusted by HCl or KOH) and added to poly-D-lysine coated glass bottom dishes (Cellvis D35-14). Poly-D-lysine coating help with immobilization of the beads. Bead was imaged by wide field microscope. Individual bead was first picked with Analyze Particle function in FIJI and saved as individual ROI. Then each ROI was analyzed by taking integrated intensity in CG channels and ATTO channels. Average G/R for >100 beads were calculated and normalized to the lowest average G/R in all samples. We notice that on the log scale normalized G/R can be approximated with a sigmoidal curve (**Extended Data Fig 1d**). This is expected response for binding-based fluorescent sensor.

For pH insensitivity we compared the sigmoidal curve at each pH from 4.5 to 7.4. From the overlay and K_d calculations, we concluded that both fold change and K_d are constant from acidic to neutral pH (**Extended Data Fig 1e**). Since the lysosome is most acidic organelle with average pH of 4.5[2]. *RatiNa* can reliably measure Na^+ in acidic organelles, and we expect to see the same Na^+ response regardless of pH.

Fig 1d is constructed from 2D plots of *RatiNa* response at 4 different pH values, i.e, pH 4.5, 5.5, 6.5 and 7.4. The individual traces are shown in **Extended Data Fig 1d** and the raw data from beads is shown in **Supplementary Fig 5b**. To assess the pH insensitivity of *RatiNa*, instead of a statistical analysis of the entire bead data, we first calculate the K_d value of Na^+ for each pH value (**Extended Data Fig 1e).** This reveals that the K_d of *RatiNa* for Na^+ is 165 mM from 4.5 to 7.4 (**Fig 1c, Extended Data Fig 1e**). The lower limit to detect Na^+ in biological systems is 5 mM.

Supplementary Note 5. *RatiNa* stability assay in macrophage lysosomes.

Lysosome is highly degrading and harbors lots of endonuclease and exonucleases[6]. Therefore, we need to test integrity of DNA backbone of *RatiNa* and find out the time when DNA is significantly degraded. We first labeled lysosomes with TMR-dextran which is not digested by lysosome enzymes. Then *RatiNa*^{AT} was targeted to lysosome with 2 h pulse and 30 min chase. Green signal from TMR-dextran will stay constant and red signal from *RatiNa*^{AT} will decrease as DNA degrades and free dye leaves lysosome via diffusion. Therefore R/G is a good indication of DNA degradation. Indeed, we observe decrease of overall red signal (**Extended Figure 2f**). We take single lysosomal R/G signal at different chase time point and plotted in histogram. (**Extended Figure 2g**). The large spread of the R/G value is due to differential uptake of dextran and DNA through fluid phase endocytosis and receptor mediated endocytosis respectively. But the R/G average indeed decreases. Previously we have shown that for 30 min chase there is minimal DNA digestion[2]. To better interpret the data, we use the following equation (2) to calculate percentage of undigested DNA (**Extended Figure 2g)**

$$lysosomal\ DNA = \frac{\left(\frac{R}{G}\right)_t}{\left(\frac{R}{G}\right)_{t_0}} \quad (2)$$

Where t = chase time and t_0 is 30 min. We decided to not measure lysosome for more than 30 min chase time to guarantee *RatiNa* sensor is not degraded.

Supplementary Note 6. *C. elegans* Na^+ clamping

We have followed previous protocol for *C. elegans* microinjection and clamping[3]. The C. elegans clamping buffer has pH 5.5 and contains 150 mM Na^+ and K^+, 150 mM Cl^-, 50 μM monensin, 50 μM nigericin, 10 μM gramicidin, 100 μM ouabain. The buffer mimicks Na^+ and K^+ level in biological system: total amount of both cation is about 150 mM. Monensin is a Na^+ ionophore, nigericin is a K^+ ionophore, gramicidin can form ion-channel like pores in membranes to facilitate Na^+ and K^+ ion exchange via diffusion[4]. Ouabain inhibits Na^+/K^+ ATPase which actively transport Na^+ and K^+ to maintain high cytosolic K^+ and low cytosolic Na^+. We chose pH 5.5 because it's close to *C. elegans* lysosome pH. Ionophores binds to Na^+ or K^+ in deprotonated form and release bound ion when protonated. Having a steep pH gradient across lysosomal membrane will make the protonation and deprotonation cycle much slower therefore pH 5.5 buffer is used.

Clamping of Na^+ proved to be challenging since the amount of Na^+ needs to be transported is in millimolar scale. After one hour of clamping we observed morphological change of *C. elegans* lysosomes from spherical to amorphous, and the effect is more severe in clamping at extreme values of 5 mM and 145 mM Na^+. We compared G/R values of clamped lysosomes and *RatiNa* beads and found indeed G/R level are very similar in both cases with slight shift in extreme values (**Fig 2d**). Therefore, we used the bead data for extrapolation of *RatiNa* calibration curve in *C. elegans* because at extreme Na^+ values clamping may not work to the fullest.

Supplementary Note 7. RAW macrophage Na^+ clamping and measurement.

RatiNa was first targeted to lysosomes. Next, cells were treated with ionophores which are added to the extracellular cell culture medium the cells are exposed to, which results in the lumenal Na^+ levels of organelles getting clamped to the value of Na^+ present in the medium or buffer. Cells are first pulsed with 1 μM *RatiNa* for 2 h and then chased for 30 min to label lysosomes. Then cells were washed with clamping buffer twice and incubated in Na^+ clamping buffer for 1h at RT prior and then imaged. Na^+ clamping buffers (150 mM NaCl/KCl, 1 mM $CaCl_2$, 1 mM $MgCl_2$, 10 mM HEPES, 5 mM glucose, pH 5.5) recapitulate cell internal osmotic pressure (321 Osm) to prevent the lysosome volume changing due to ion exchanges. 50 μM monensin, 50 μM nigericin, 10 μM gramicidin are used as Na^+ and K^+ ionophores to clamp Na^+ and K^+ and 100 μM of ouabain is used to inhibit cell surface Na^+/K^+ ATPase activity to facilitate clamping.

Unlike *C. elegans* coelomocyte which can accumulate almost all injected DNA in lysosomes, cultured cells uptake less DNA and the overall fluorescence signal is weaker. A new calibration curve is required for measurements in macrophage lysosomes. Clamping buffer we used for macrophage is pH 5.5, 150 mM Na^+ and K^+, 150 mM Cl^-, 5mM D-glucose, 1 mM $MgCl_2$, 1 mM $CaCl_2$, 10 mM HEPES, 50 μm monensin, 50 μm nigericin, 10 μm gramicidin, 100 μm ouabain[5]. The buffer is slightly different from *C. elegans* clamping buffer and better recapitulate internal osmolarity of cultured cells, prevent cells from swelling or shrinking. With similar workflow we clamped macrophage lysosomes and attempted to image *RatiNa* in Na^+ clamped lysosomes. We noticed that CG signal is very low and G/R fold change from lysosomes are only ~2 fold compared to ~4 fold from *C. elegans* measurements.

In order to show that *RatiNa* can reliably measure Na^+ in macrophage lysosomes, we looked into the difference of *RatiNa* fold change in macrophages. First, we observed that autofluorescence can be detected at the optimal excitation and emission wavelength of CG in macrophages (**Extended Fig 2e)** Then we looked that *RatiNa*^{AT} in macrophages in both CG channel and ATTO channel. We observe signal in both channels and if ROI is picked from ATTO channel and G/R is calculated for *RatiNa*^{AT} containing lysosomes, a non-specific G/R signal is obtained even without the CG dye (**Extended Fig 2e, 2g**). And if the averaged non-specific G/R signal is subtracted from G/R from clamped lysosomes, we can get fold change of ~3.5 fold from 5 mM to 145 mM Na^+, which is similar to *C. elegans* clamped lysosomes. we identify and exclude those ROIs where the G channel is less than or equal to autofluorescence levels (very few, <5%). Thus, all the lysosomal Na^+ values are from those ROIs with clear signal in both G and reference R channels, effectively excluding imaging artifacts. We concluded that even though fold change is less in macrophages we can still get a linear calibration curve with the Na^+ clamping value. The new calibration line should be used for all RAW macrophage lysosome Na^+ measurement.

Supplementary Note 8. Colocalization analysis of *RatiNa^{AT}* in *C. elegans* early endosome, late endosome, and lysosome

RatiNa targets organelles through scavenger receptor mediated endocytosis. Endocytosis is a time dependent process and cargo is trafficked to early endosome then to late endosome and finally to lysosome. If we image at specific chase time *RatiNa* can be found localized majorly in early endosome, late endosome or lysosomes. We have previously established these timepoints in *C. elegans* with other DNA based sensors[7,8]. Now we need to determine the effectiveness and specificity of *RatiNa* targeting using these timepoints. For early endosome targeting we used *cdIs131* worm which express GFP::RAB-5 fusion protein in coelomocytes. RAB-5 is an early endosome marker protein. 5 min after injecting cdls131 worm with *RatiNa^{AT}*, worms were imaged and colocalization was determined as described in methods. For late endosome targeting we used *cdIs66* mutant worms which express GFP::RAB-7 fusion protein in coelomocytes. RAB-7 is a late endosome marker protein. 17 min after injecting cdls66 worms colocalization of *RatiNa^{AT}* to late endosome is determined. For lysosome targeting we used *pwIs50* mutant worms which express GFP with LMP-1 promoter. LMP-1 is a lysosome marker protein. 60 min after pwls50 worms colocalization of *RatiNa^{AT}* to lysosome is determined. As shown in **Extended Data Fig 3a***, RatiNa* is localized to early endosome, late endosome and lysosome with high efficacy at 5 min, 17 min and 60 min respectively. Next, we check anti-colocalization with other endocytic organelles. *RatiNa* is trafficked from early endosome to late endosome, so it is required to show at 5 min there's no colocalization to late endosomes. Indeed, there is little colocalization of *RatiNa* with RAB-7 at 5 min post injection (**Extended Data Fig 3b**). Similarly anti-colocalization with early endosome should be shown for late endosome targeting and there is little colocalization of *RatiNa* with RAB-5 at 17 min post injection (Supplementary Figure 9b). RAB-7 partially labels lysosome, so it is not a great marker for anti-colocalization. Therefore, we used LMP-1 anti-colocalization at 17 min to show specificity of lysosome targeting (**Extended Data Fig 3b**).

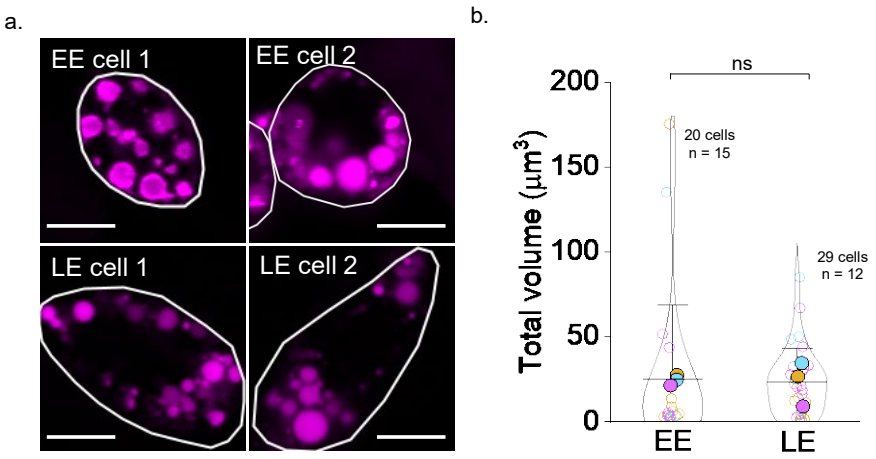

Supplementary Figure 6. EE and LE Na^+ difference is not due to volume change
a. Representative images of EE and LE in *C. elegans*. Only reference fluorophore channel is shown to show the size of endosomes. b. total volume of all endosomes was calculated for each coelomocyte cells. Two sample *t*-test shows no significance. And less Na^+ in LE is not due to a volume change. Error bar represents SD. Two sample two-tailed t-test was used for statistical analysis assuming equal variance. P = 0.89.

Supplementary Note 9. Analysis of volume of endosomes
Volume of endosomes was calculated as follows: First, all endosomes are labeled with ROI exactly around the edge manually. This step is done for Na^+ level analysis as well. Second, "Measure" function of ImageJ was used to give output of area of ROI in micrometers (A). Next, we assume all endosomes are spherical in shape and calculate the volume of endosomes by the following formula (1):

$$V = \frac{4}{3}\pi\left(\frac{A}{\pi}\right)^{\frac{3}{2}} \quad (1)$$

Then we add volume of all endosomes of a given stage (i.e., EE or LE) in a cell together and compare total endosome volume per cell in μm^3.

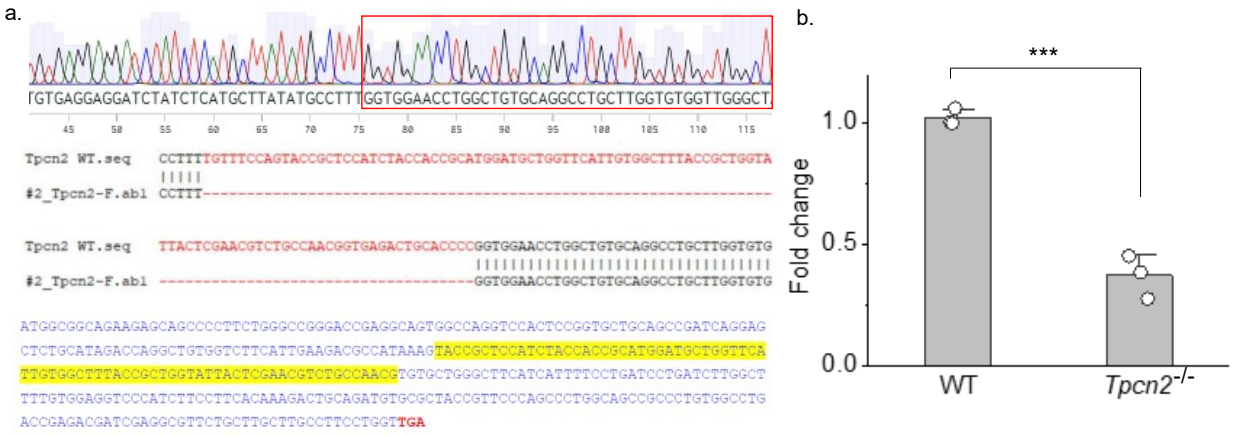

Supplementary Figure 7. Confirmation of *Tpcn2* KO in RAW macrophages

a. Genomic sequencing data of CRISPR KO *Tpcn2* null RAW macrophages (upper panel). Red rectangle indicates site of deletion. Alignment of WT and KO cells shows the full 101 bp homozygous deletion in red font (middle panel). In the full cDNA sequence (lower panel) 77 bp deletion is shown in yellow highlight. Base editing cased an early stop codon in *Tpcn2* mRNA. b. qRT-PCR analysis of *Tpcn2*$^{-/-}$ RAW macrophage and WT RAW macrophages shows low level of mRNA. *Gapdh* is used as reference gene. Data are presented as mean values + SD from n = 3 independent experiments. Two sample two-tailed t-test was used for statistical analysis assuming equal variance. P = 2.9E-4

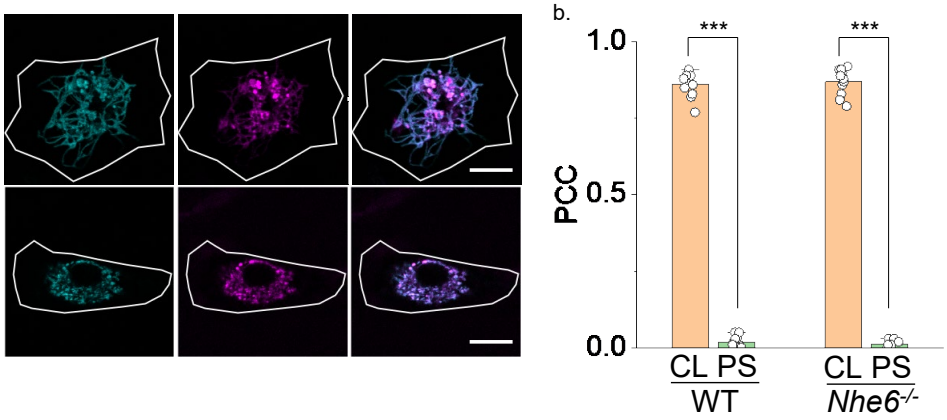

Supplementary Figure 8. Lysosomal targeting of *RatiNa^{AT}* in primary mouse BMDM
a. Representative images of RatiNa^{AT} colocalizing with mouse BMDM lysosome labeled with TMR-dextran. 30 min and 45 min chasing time are required for lysosomal localization for WT and *Nhe6$^{-/-}$* BMDM respectively. b. Lysosomal colocalization quantified with PCC. CL, colocalization, PS, Pixel shifted image. Data are represented as mean + SD from n = 11 cells. Two sample two-tailed t-test was used for statistical analysis assuming equal variance. P = 2.6E-24, 1.5E-24 for WT and *Nhe6$^{-/-}$*.

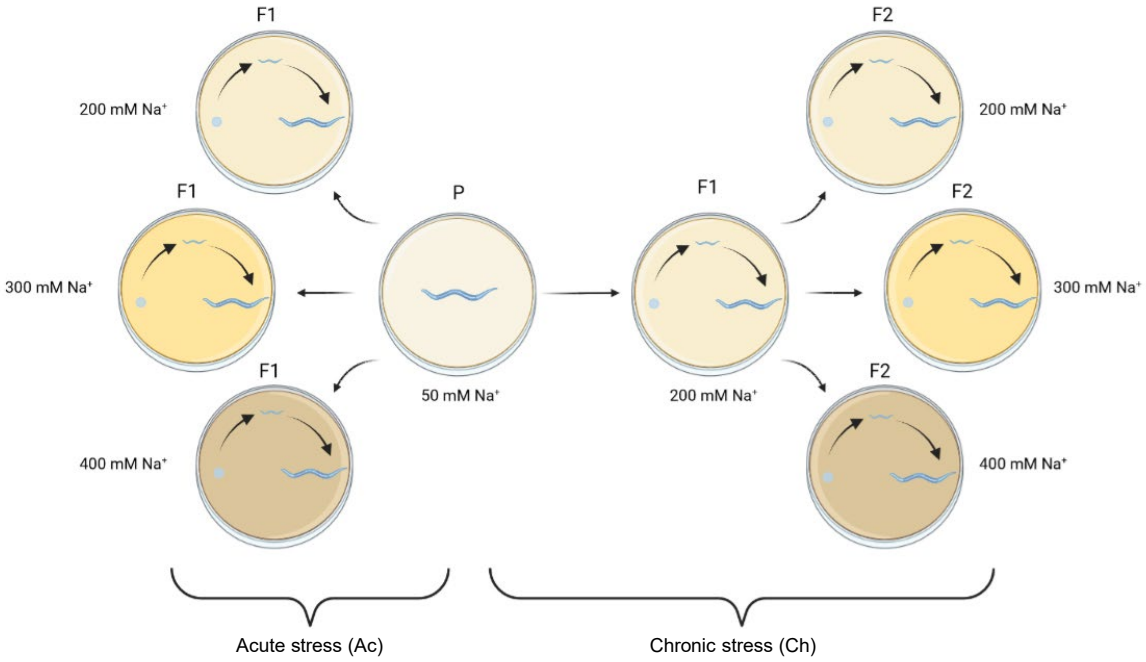

Supplementary Figure 9. Workflow of brood size assay for salt stress
Brood sizes were used to compare salt stress tolerance of different worm mutants. For acute stress (Ac), worms were directly transferred to high Na^+ plates from NGM plate and brood size counted. For chronic stress (Ch), worms were grown for one generation at 200 mM Na^+. Then stressed worms were transferred to high Na^+ plate and brood size was counted.

Supplementary Note 10. *C. elegans* Na^+ stress assay
C. elegans can respond to high environmental salt through physiological remodeling[9], which allows them to tolerate lethal level of salt. Most mutants show a normal life cycle, with no obvious lysosome morphology defects. We hypothesized that lysosomal Na^+ defects may become prominent under conditions of Na^+ stress or overload.

First, we subjected different Na^+ transporter mutant worms to salt stress. At 400 mM Na^+ which is previously described as lethal, worms are still alive albeit with no movement and only move when poked with platinum wire. Therefore, we decided to score the salt stress response with a brood size assay instead of survival assay (**Supplementary Fig 9**) 5 L4 worms were transferred to high Na^+ plates with 200 – 400 mM Na^+ and allowed to make progeny. After 24 hours the original worms were removed from the plate and the progeny were allowed to grow into L3-L4 stage for counting. First, we confirmed that all worms can respond to high Na^+ stress to some extent. This is shown by the increase of progeny count from Ac to Ch worms. (**Extended Data Fig 4a)**. However, Na^+ transporter mutants cannot tolerate stress as well as N2 worms, shown in 400 mM Na^+ experiment where only N2 worms tolerate Ac stress to give progeny. Notably *nhx-5(-)* worms were most susceptible to salt stress, had the biggest perturbation in lysosomal Na^+, indicating lysosomal Na^+ plays an important role in the salt stress adaptation process.

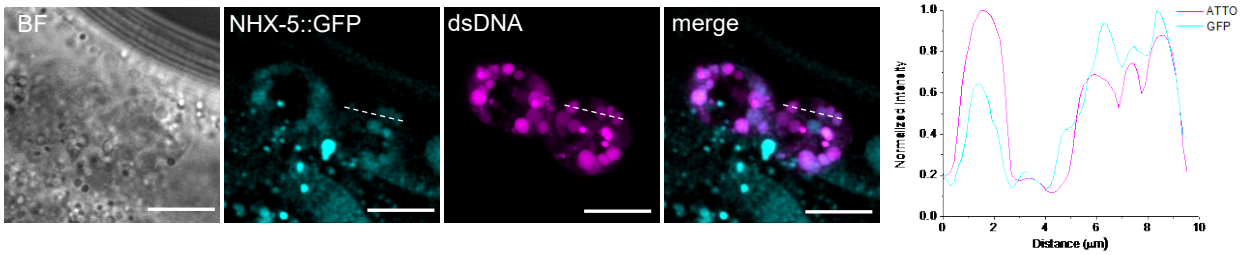

Supplementary Figure 10. NHX-5 is found in coelomocyte lysosomes
a. NHX-5::GFP is overexpressed in N2 worms by extrachromosomal array. *RatiNa*^{AT} is injected and 1 h chase time is used for lysosome labeling in coelomocytes. Low level of NHX-5 can be found in coelomocyte lysosomes. b. line profile colocalization analysis of NHX-5::GFP and *RatiNa*^{AT} shows NHX-5 can be found in coelomcyte lysosomes. Images are representative of n = 12 worms in 2 independent experiments.

Supplementary Note 11. Extrachromosomal array expression of NHX-5::GFP
To show the localization of NHX-5 in coelomocyte lysosome we choose to overexpress NHX-5::GFP with native *nhx-5* promoter. Plasmid with NHX-5::GFP is a gift from Prof. Keith Nehrke[10] described in the method section. Nehrke et al. found that NHX-5 is localize in subcellular compartment and showed most expression lumbar ganglion near the tail[10]. In our extrachromosomal array expression experiment, we observed a very low level of GFP signal in the coelomocytes (**Supplementary Fig 10**). We injected *RatiNa*^{AT} and performed colocalization experiment with NHX-5::GFP. In a small population of injected worms (4/16) we found colocalization of *RatiNa*^{AT} with NHX-5::GFP.

Supplementary Note 12. Lysosomal Na^+ measurement for *nhx* mutant worms.
NHX proteins are Na^+/H^+ exchangers and many have been previously shown to localize in intracellular compartments, even though specific organelles are not mentioned[10]. We obtained NHX deletion mutant worms from CGC and measured lysosomal Na^+ measurement in mutant worms (**Extended Data Fig 4b,d**). Some NHX mutants have slightly lower Na^+. *nhx-5(-)* worms show very low Na^+ indicating NHX-5 facilitates lysosomal Na^+ import. NHE6 is the closest human orthodox to *C. elegans* NHX-5[11] (41% identity, 60% similarity, aligned with 84% sequence coverage). The closest homolog of worm NHX-7 is human NHE1 (35% identity, 55% similarity, aligned with 77% sequence coverage), which is a plasma membrane protein. Lysosomal Na^+ in *nhx-8(-)* worms is unaffected. Its closest homolog is NHE8 (48% identity, 69% similarity, aligned with 61% sequence coverage), which is found mainly in TGN. We measured lysosomal Na^+ in acutely stressed N2 and mutant worms. Intriguingly, upon acute Na^+ stress, all mutant worms show higher lysosomal Na^+ while N2 worms show lower lysosomal Na^+.

Supplementary Table 1. Design and Sequence of all *RatiNa* probes and *Bromo I-switch*

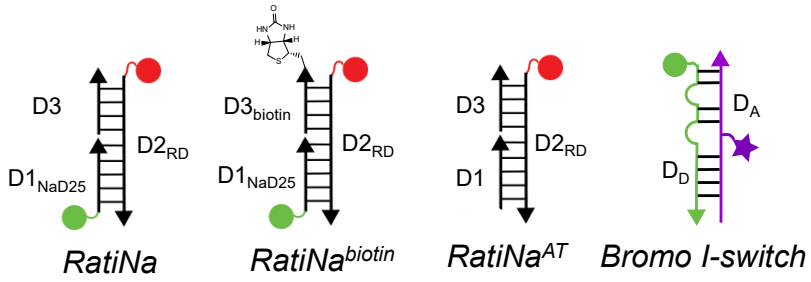

name	sequence
$D1_{NaD25}$	5'-CG-ATC AAC ACT GCA TAT ATA TAC GAC C-3' (25mer)
D1	5'-ATC AAC ACT GCA TAT ATA TAC GAC C-3' (25mer)
$D2_{RDL}$	5'-ATTO647N-C ACT GCA CAC CAG ACA GCA A G GTC GTA TAT ATA TGC AGT GTT GAT-3' (45mer)
$D3_{biotin}$	5'-T TGC TGT CTG GTG TGC AGT G-BioTEG- 3' (20mer)
D3	5'-T TGC TGT CTG GTG TGC AGT G – 3' (20mer)
D_D	5'-Alexa488N-CCC CT AAC CCC TAA CCC CTA ACC CCA TAT ATA TCC TAG AAC GAC AGA CAA ACA GTG AGT C-3' (60mer, C = 5-Br-dC)
D_A	5'-GAC TCA CTG TTT GTC TGT CGT TCT AGG ATA-iAlex647N-AT ATT TTG TTA TGT GTT ATG TGT TAT-3' (60mer, iAlex647N = Alexa647N labeled T)

References

1. Martin, V. V., Rothe, A. & Gee, K. R. Fluorescent metal ion indicators based on benzoannelated crown systems: a green fluorescent indicator for intracellular sodium ions. *Bioorg Med Chem Lett* **15**, 1851–1855 (2005).
2. Suresh, B. *et al.* Tubular lysosomes harbor active ion gradients and poise macrophages for phagocytosis. *PNAS* **118**, (2021).
3. Surana, S., Bhat, J. M., Koushika, S. P. & Krishnan, Y. An autonomous DNA nanomachine maps spatiotemporal pH changes in a multicellular living organism. *Nat Commun* **2**, 340 (2011).
4. Sorochkina, A. I. *et al.* N-Terminally Glutamate-Substituted Analogue of Gramicidin A as Protonophore and Selective Mitochondrial Uncoupler. *PLOS ONE* **7**, e41919 (2012).
5. Ishiguro, H., Steward, M. C., Lindsay, A. R. & Case, R. M. Accumulation of intracellular HCO3- by Na(+)-HCO3- cotransport in interlobular ducts from guinea-pig pancreas. *The Journal of Physiology* **495**, 169–178 (1996).
6. Trivedi, P. C., Bartlett, J. J. & Pulinilkunnil, T. Lysosomal Biology and Function: Modern View of Cellular Debris Bin. *Cells* **9**, 1131 (2020).
7. Saha, S., Prakash, V., Halder, S., Chakraborty, K. & Krishnan, Y. A pH-independent DNA nanodevice for quantifying chloride transport in organelles of living cells. *Nature Nanotechnology* **10**, 645–651 (2015).
8. Narayanaswamy, N. *et al.* A pH-correctable, DNA-based fluorescent reporter for organellar calcium. *Nature Methods* 1 (2018) doi:10.1038/s41592-018-0232-7.
9. Lamitina, S. T., Morrison, R., Moeckel, G. W. & Strange, K. Adaptation of the nematode Caenorhabditis elegans to extreme osmotic stress. *American Journal of Physiology-Cell Physiology* **286**, C785–C791 (2004).
10. Nehrke, K. & Melvin, J. E. The NHX Family of Na+-H+ Exchangers in Caenorhabditis elegans *. *Journal of Biological Chemistry* **277**, 29036–29044 (2002).

11. Kim, J. *et al.* NHX-5, an Endosomal Na+/H+ Exchanger, Is Associated with Metformin Action. *J Biol Chem* **291**, 18591–18599 (2016).